

# A Facile Synthesis of Nanophase Cadmium Sulfide Semiconductor

Sanjoo Yadav<sup>1</sup>, Ashok Kumar<sup>2</sup>

<sup>1,2</sup>Department of Physics, H.D. J. College, Veer Kunwar Singh University, Ara

<sup>2</sup>Corresponding Author Email: [dr.ashokkumar250259\[at\]gmail.com](mailto:dr.ashokkumar250259[at]gmail.com)

**Abstract:** *Physical properties of materials are independent of the sizes when the sample is bulk, but start depending on the particle sizes of nanometer (nm). Especially, binary semiconductors show controllable multifunctionality in a single system, like magnetism and opto-transparency in semiconductors suited for spin-based electronics. Cadmium sulfide and stannic oxide nanoparticles are such perspective materials. In this work, we report a facile green synthesis of undoped nanophase CdS, characterized by X-ray diffraction, SEM, and uv-vis spectroscopy. It crystallizes in the cubic unit cell of edge  $a=b=c=0.5796$  nm with a microstrain of -0.022 in a mean particle size of about 2 nm as observed by Williamson-Hall plots. The uv-vis absorptions data generate Tauc Plots giving the optical band gaps of 2.64eV in the reference. Its microstrain and defects may have magnetic consequences.*

**Keywords:** Nanophase, microstructure, cadmium sulfide, stannic dioxide, Tauc plots

## 1. Introduction

Recent literature survey shows the possibility of ferromagnetic order in nanoparticles without using magnetic elements in oxides and sulphides. As known, ideal bulk cadmium sulfide has closed orbits, and hence should exhibit diamagnetism. However, experimental evidence defies the expectation. Magnetic behaviour observed have possibly their link with spin-spin interactions. The spin-based magnetic materials may be antiferromagnetic (discovered by Neel, 1930), ferrimagnetic (discovered in 1948), and spin-canted materials: canted-antiferromagnetic, canted ferrimagnetic, and ferromagnetic and superparamagnetic materials. Different kinds of magnetic effects may cooperate in materials and a single system may show more than one magnetic phase under different external pressures, temperatures, and fields. Quantum theoretic exchange interaction arising out of wavefunction overlaps – direct or indirect – explains several of these effects. Ruderman-Kittel-Kasuya-Yosida (RKKY) interaction represents an interaction of distant magnetic ions mediated by mobile electrons, also known as super-exchange interaction. Anderson modified it by the idea of hopping electrons between ions through the oxygen ion. The strength of these interactions is much greater than dipolar interaction. These mechanisms are linked to anisotropy feature of magnetic materials. Magnetic anisotropy is linked to microstrains in crystals, which develop in crystals due to deviations in lattice parameters, and possibly creates ferromagnetic order as observed in sulphide nanoparticles. Magnetic properties in oxide and sulphide samples arise due to anion defects also. Undoped stannic dioxide exhibits ferromagnetism. CdS is also observed to show ferromagnetism [1]. The synthesis procedure affects the microstructure and magnetic behaviour, and is challenging.

There are several methods of nanoparticle synthesis in literature such as spray pyrolysis or flame spray synthesis [2, 3], laser removal process [4], mini arc plasma [5], hydrothermal [6, 7], amorphous citrate route [8], wet chemical method [9], solid-state reaction [10], sol-gel [11, 12], co-precipitation [13], and so on. On nano-scale,

particles show interesting properties because of quantum confinement and parameters of microstructures. The binary compound we worked on is cadmium sulfide which can have hexagonal wurtzite and cubic structure. In this work, CdS nanoparticles were synthesized in a facile chemical route using passivator EDTA and the method rendered the formation of cubic unit cells.

## 2. Experimental Method

For co-precipitation method to proceed upon, chemicals of analytic grade were procured for direct uses. The chemicals for the two kinds of samples were Hydrated cadmium sulfate, sodium sulfide hydrate, and ethyl di-amide tetra-acetic acid di-sodium hydrate to synthesize quantum dot cadmium sulfide. For the other sample, the directly procured chemicals stannic chloride penta-hydrate, ammoniacal solution, and de-ionized water were used and the nanophase stannic oxide was prepared, as described in the following.

As in Chart (Figure 1), 25 mL solution of 7.695 g cadmium salt in DI water was freshly prepared. A mass of 0.971 g of sodium sulfide salt was dissolved in DI water to get a solution of 25 mL. Further procedures are given in the flow chart. The solutions were mixed in beaker kept on a hotplate with a magnetic stirrer and a temperature reader. The magnetic stirrer was used for homogenizing and hotplate for warming the new solution to 40degree C for 1 hour. A burette already containing EDTA-di sodium solution, was used in this period for its dropwise addition at 40 drops a minute, as a pH controller.

A vacuum oven and desiccator were used for thermal treatment at more than boiling points of solvents. The CdS-sample was obtained at an annealing temperature of 170°C. Final cooling was done in open to room temperature.

The sample was characterized using modern machines.

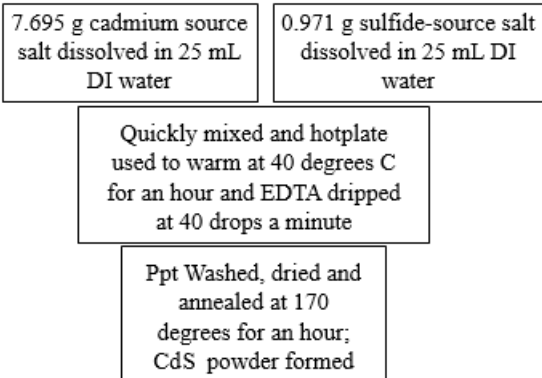


Figure 1: Chart of Co-precipitation method

### 3. Results and Discussion

#### Microstructural Characterization

The powder samples obtained were characterized using x-ray diffraction. WH plot was drawn and unit cell, microstructure, and microstrains were determined. XRD pattern of the sample was obtained using copper k-alpha radiation of wavelength 1.541 angstroms on RIGAKU MINI FLEX 600 at a scan rate of 2 degrees per minute in steps of 0.02 degrees. XRD plot in Figure 2 shows line broadening that indicates nanosized particles in the sample, and may be involving other sources of broadening like microstrains, extended defects, crystalline domain sizes and distribution of domains.

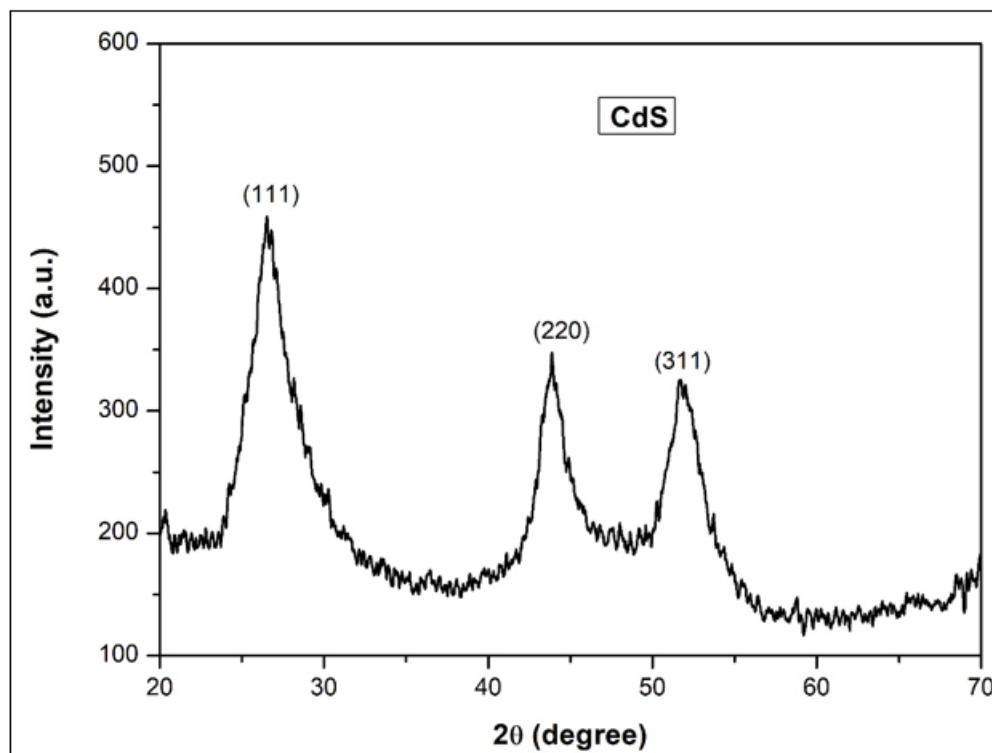


Figure 2: XRD pattern of cadmium sulfide sample

Bragg's law for strong maxima is given by

$$2d_{hkl} \sin \theta_{hkl} = \lambda \quad (1)$$

The lattice parameters of a cubic unit cell are given by

$$\frac{1}{d_{hkl}^2} = \frac{h^2 + k^2 + l^2}{a^2} \quad (2)$$

The lattice parameters obtained are  $a = b = c = 5.796 \text{ \AA}$ .

Table 1: Lattice parameters

Miller indices	$2\theta_{hkl}$	Lattice parameter, nm	Mean, a nm
111	26.85583	0.5745	0.5796
220	44.15067	0.5796	
311	51.80718	0.5848	

Peak broadening arising out of crystallite sizes only is used to find the particle mean size. This effect was considered by Scherrer and others [14]. We have

$$\beta \cos \theta = k\lambda/D \quad (3)$$

We used the XRD plot to measure full width at half- the-maximum of the most intense peak,  $\beta$ , in radian, and half-

the-angular position of the intense peak,  $\theta$ . The shape factor  $k$  is close to 1.

The crystalline sizes given by equation (3) were further considered for other sources of peaks broadening. Stokes and Wilson [15], Williamson and Hall [16], and others studied the effect of defects in the form of microstrain in unit cell that affects the peak width. The equation (3) gets modified in usual symbols to take into account the microstrain, as of follows:

$$\beta_{hkl} \cos \theta_{hkl} = \frac{k\lambda}{D} + 4\epsilon \sin \theta_{hkl} \quad (4)$$

We measured the angular positions of peaks and their full widths at half-the-maxima using the XRD plots. In the WH plot of equation (4), a linear fit was used to get the slope and intercept (Figure 4). Mean size of nanoparticles was obtained from the intercept, and the microstrain from the slope.

$$\frac{k\lambda}{D} = 0.08272$$

For wavelength of 1.541 angstrom, and k of 0.94, we get D is 1.75 nm. The particle seems compressed as the microstrain is - 0.02208.

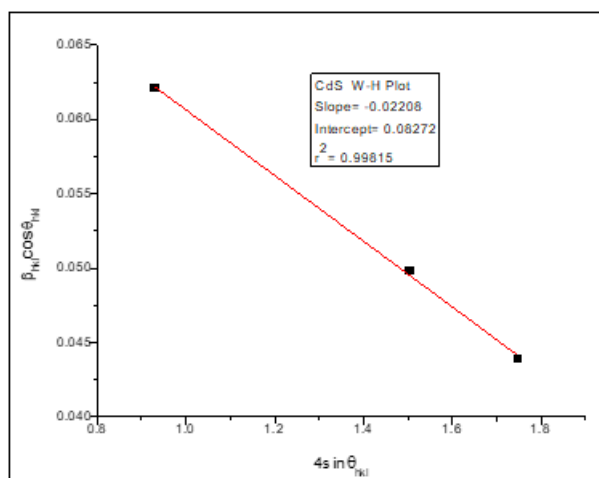


Figure 3: WH plot of sample

### SEM studies

The samples was studied for their morphology by scanning electron microscopy. The micrograms are exhibited in Figures 4. A size distribution and agglomeration of spherical nanoparticles is observed.

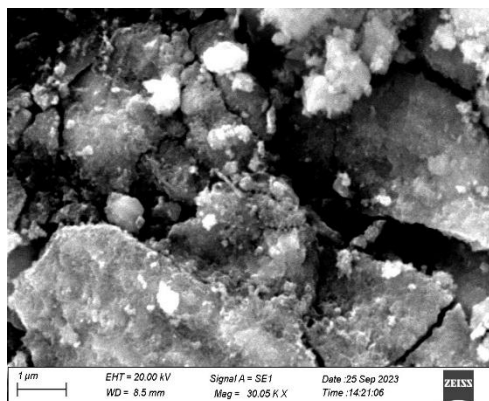


Figure 4: CdS sample

### Band gap studies using UV spectroscopy

The samples are characterized by ultraviolet-visible spectroscopy for absorbance. If I be the incident intensity and I' be the transmitted intensity through the sample in cuvette of length L, the Beer-Lambert law gives the relation

$$I' = I \exp(-\alpha L) \quad (5)$$

The quantity  $\alpha$  is absorption coefficient.

Taking common logarithm,

$$\log \frac{I}{I'} = \alpha L \log e$$

The RHS is defined as absorbance, A, measured in uv-vis spectroscopy as a function of wavelength, and L= 1 cm is standard laboratory value of for cuvette. Thus,

$$2.302 A = \alpha \quad (6)$$

The optical band gap,  $E_o$ , the upper threshold of radiation that can be absorbed, is given by Tauc relation [17]:

$$(\alpha h\nu)^n = B(h\nu - E_o)$$

For the allowed dominant interband transitions, direct band transition, we have  $n=2$ , and for indirect band  $n=1/2$ . For our samples  $n=2$ . Hence

$$(\alpha h\nu)^2 = B(h\nu - E_o) \quad (7)$$

Equation (7) is graphically solved in the region of the LHS that matches the linear part of the graph of RHS, whose extrapolation intersects the abscissa at the band gap,  $E_o$ . For CdS, it is 2.64 eV [18].

### 4. Conclusion

Nanophase cadmium sulfide is successfully prepared. The XRD patterns and the lattice parameters are consistent with the standard values given in JCPDS file. Very small sizes of the few nm make them very reactive and sticking as shown in their SEM images. Smallness of sizes leads to quantum confinement, and blue shift in optical band gap determined from UV-spectra driven Tauc plots.

### References

- [1] N. Susha, Ajith S. Kumar, S. Vivek, Swapna. S. Nair, 'Defect induced magnetism in green synthesized Cadmium Sulfide nanoparticles for spintronics applications, *Material Science and Engineering*, vol 265, (2021).
- [2] Liu W and H Wang, *Journal of Materiomics*, **6**, 385-96(2020)
- [3] T Sahm, L Madler, A Gurlo, N Barsan, S E Pratsinis, and U. Weimar, *Sens. Actuators B*, **81**,165-169 (2004)
- [4] F Paraguay-Delgado, W Antunez-Flores, M Miki-Yoshida, A Anguilar-Elguezabal, P Santiago, R Diaz and J A Ascencio, *Nanotechnology*, **16** 688 (2005).
- [5] G Lu, K L Huebner, L E Ocola, M G Josifovska, and J Chen, *J. Nanomaterials*, 1-7(2006)
- [6] S Fujihara, T. Maeda, H Ohgi, E Hosono, H. Imai, and S H Kim, *A Chem. Society*, **20**, 6476-6481(2004)
- [7] F Shaikh et al, *Powder Technol.* **326**, 479-87 (2018)
- [8] M Bhagwat, P. Shah, V. Ramaswamy, *Materials Letters*, **57**, 1604-1611(2003)
- [9] S Gnanam and V Rajendran, *Digest Journal of Nanomaterials and Biostructures*, **5**, 699-704(2010)
- [10] F. Li, J. Xu, X. Yu, L Chen, J. Zhu, Z. Yang and X. Xin, *Sens. Actuators B*, **81**, 165-169 (2002)
- [11] L.L. Hench and J K West, *Chem. Rev.*, **90**, 33-72(1990)
- [12] L P Wang et al, *Adv. Mater.* **29**, 1603286 (2017)
- [13] G. Lu et al, *Sens. Actuators B: Chemical* **162**, 82-8(2012)
- [14] P. Scherrer, *Gottinger Nachrichten Gesell.* **Vol 2**, p98 (1918)
- [15] A R Stokes and A J C Wilson, *Proc. Phys. Soc.* **56**, 174 (1944)
- [16] G K Williamson and W.H. Hall, *Acta Metall.* **1**, 22-31 (1953)
- [17] Tauc J, *Materials Research Bulletin*, **3**, 37-46(1968)
- [18] Sultani, N., et al, *Int. J. Mol. Sci.*, **13**, 12242-58 (2012)